Observation of Two Glass Transitions in a Thermotropic Liquid-Crystalline Polymer

Juan P. Fernández-Blázquez, Antonio Bello, and Ernesto Pérez*

Instituto de Ciencia y Tecnología de Polímeros (CSIC), Juan de la Cierva 3, 28006 Madrid, Spain

Received April 1, 2004; Revised Manuscript Received September 15, 2004

ABSTRACT: DSC and real-time variable-temperature synchrotron experiments have been performed on a thermotropic poly(etherester), PH31B32, with biphenyl units as mesogens and spacers with methyl substituents. It has been found that PH31B32 develops a low-ordered SmCalt mesophase with a rather slow rate of formation in such a way that the isotropic melt of this polymer can be easily quenched into the glassy amorphous state at the usual cooling rates of the calorimeter. Considerably high annealing times at temperatures above T_g are necessary to develop such a mesophase. The extent of transformation and symmetry of the mesophase have been determined by means of calorimetric and X-ray diffraction experiments. The DSC results show that the glass-transition temperatures of the amorphous and liquid-crystalline states are clearly different: 95 and 84 °C, respectively. Moreover, the results show that the isotropization temperature increases linearly with the annealing temperature (the temperature at which the mesophase has been formed). The synchrotron experiments show that the mesophase layer spacing is slightly lower for the higher annealing temperatures, indicating a slightly more compact structure. Although the WAXS profiles of the two phases (mesophase and amorphous) are rather similar, the mesophase has noticeably smaller most probable intermolecular distances and a smaller width of the WAXS broad peak. The temperature coefficients of these intermolecular distances are also different for the various phases, and clear discontinuities are observed at the glass transitions. The corresponding values of T_g obtained from these results are 94 and 84 °C for the amorphous and liquid-crystalline phases, respectively, in perfect agreement with the DSC results. The correlation lengths estimated from the widths of the mesophase layer peaks are of the order of the extended chain length of the polymer, so that no extensive chain folding seems to be present in the mesophase of PH31B32. This fact will favor the attainment of high degrees of liquid crystallinity. Moreover, the higher correlation lengths deduced for the higher annealing temperatures point to a segregation of defects from the smectic structure in a greater extent, which may explain the corresponding higher isotropization temperatures.

Introduction

Liquid-crystalline polymers, LCPs, are a subject of increasing interest due to the favorable combination of key properties such as strength, easy flow, excellent dimensional stability, ability to incorporate high levels of fillers, excellent chemical resistance, and remarkably low gas permeability.[1] Moreover, a wide range of properties can be obtained in LCPs with simple chemical variations in their structure, so that these materials are very good models to investigate the influence of such variations on the final properties.

LCPs usually exhibit extensive polymorphism, and one of their more interesting features is the possibility of freezing the orientational order of the mesophase just by cooling the sample at temperatures lower than the glass transition, T_g, which is an attractive way to obtain anisotropic glasses with unique optical, mechanical, or electrical properties.[2]

The analysis of the polymeric behavior in these glassy systems must take into account special effects deriving from the presence of orientational order, and therefore, it can show special characteristics differing from those found in classical amorphous polymers. In the case of the glass transition, for instance, activation of the segmental motion at temperatures above T_g must be strongly related to the rotational freedom of the mesogens, which at the same time has to be compatible with the symmetry of the mesophase. Despite extensive interest in the solid-state physics of LCPs, there are not many examples in the literature dealing with differences in the properties of the amorphous and liquid-crystalline glasses of thermotropic main chain LCPs.[3−9] The existence of two different glass transitions for the liquid-crystalline and amorphous states, the former laying at lower temperatures than the later, has been suggested by some authors regarding DSC and dielectric and dynamic-mechanical spectroscopy measurements. However, only a few studies in suitable systems have been performed.

The reason for the existence of few studies lies in the fact that it is usually very difficult in LCPs to avoid the formation of the mesophase with regular quenching conditions. Thus, although in principle glassy amorphous states can be obtained by supercooling the isotropic melt, avoiding the formation of the mesophase, however, for most LCPs the quenching of the melt is not possible even at very fast cooling rates because of the rapid kinetics of the liquid-crystallization process. To slow it down, the tendency of the elongated LCP chains to build the supramolecular structure must be reduced by, for example, decreasing their structural and geometrical symmetry. This can be attained, for instance, in polymer systems where the mesogens are biphenyl units and using odd spacers with methyl substituents. It is known that polybibenzoates with linear odd spacers show a smectic mesophase of the type SmCalt, where consecutive mesogens are arranged in an alternating antiparallel fashion.[10−18] This reduction of the geometrical symmetry of the molecule diminishes

* To whom correspondence should be addressed. E-mail: ernestop@ictp.csic.es.

10.1021/ma049354r CCC: $27.50
Published on Web 10/29/2004

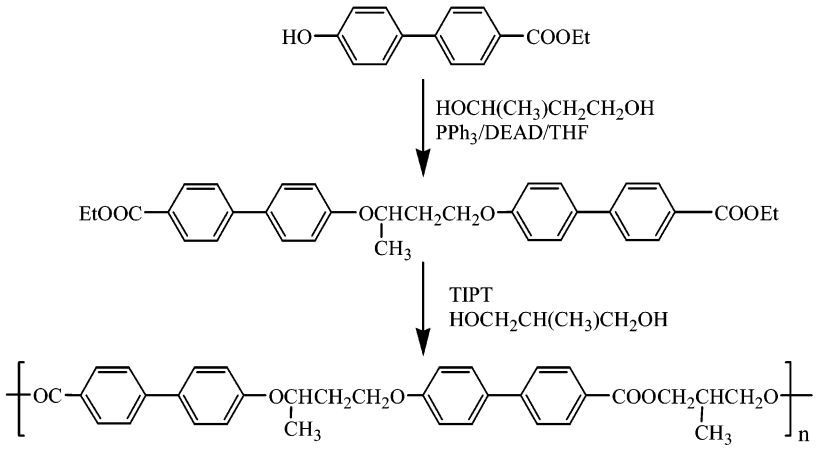

Figure 1. Synthesis and structural unit of PH31B32.

the self-assembly tendency of the mesogens to build the supramolecular ordering. In addition, the methyl group introduces structural irregularity not only because of the lowering of the interchain interactions,[19,20] but also because of the random distribution of head-to-head and head-to-tail sequences along the polymer backbone. Evidently, if the reduction of regularity is too high, the polymer system may loose the ability to produce mesophases (or any other kind of regular structures).

The aim of the present work is to synthesize a new main-chain LCP with sufficient (but not too many) structural and geometrical irregularities to be able to observe, independently, the glassy states of both the amorphous and the liquid-crystalline phase to analyze the corresponding similarities and/or differences between them. For that purpose, DSC and real-time synchrotron X-ray experiments have been carried out.

Experimental Section

Synthesis. The monomer for the synthesis of the polymer was obtained from ethyl 4′-hydroxy-4-biphenylcarboxylate and (*R*,*S*)-1,3-butanediol under Mitsunobu conditions,[21] reaction that gives good yields. The detailed procedure for the synthesis of this compound is as follows.

1,3-Bis(4-diethyloxycarbonyl-4′-biphenyloxy)-1-methylpropane. Triphenylphosphine (5,5 g, 20 mmol), ethyl-4′-hydroxy-4-biphenylcarboxylate (5 g, 20 mmol), and (*R*,*S*)-1,3-butanediol (0,9 g, 10 mmol) were dissolved in 60 mL of anhydrous tetrahydrofuran. Diethyl azodicarboxylate, DEAD (3,5 g, 12 mmol), was added to the mixture dropwise with stirring at room temperature. The mixture was left overnight. The solvent was evaporated in vacuo, and the product was purified by flash chromatography using silica gel with dichloromethane/hexane 5:1 as eluent. Yield 65%.

^{1}H-RMN ($CDCl_3$): δ 1.39 (t, 6H, C**H$_3$**CH_2), 1.41 (d, 3H, C**H$_3$**-CH), 2.03−2.25 (m, 2H, C**H$_2$**CH_2O), 4.08−4.24 (m, 4H, C**H$_2$**-OPh), 4.37 (q, 4H, OC**H$_2$**CH_3), 4.68−4.80 (m, 1H, C**H**(CH_3)), 6.94−8.10 (m, 16H, H_{ar}).

^{13}C-RMN ($CDCl_3$): δ 14.34 (**C**H_3CH_2), 19.91 (**C**H_3CH), 36.31 (**C**H_2CH_2O), 60.87 (O**C**H_2CH_3), 64.36 (CH_2**C**H_2O), 70.77 (**C**H-(CH_3), 114.89; 116.21; 126.37; 128.33; 128.40; 128.53; 130.02; 132.47; 145.02; 158.20; 159.01 (24C_{ar}); 166.55 (**C**OOCH_2CH_3).

Polymerization. The polymer was obtained by melt transesterification of the monomer with 2-methyl-1,3-propanediol using tetraisopropyl titanate, TIPT, as catalyst.[19,20] The polymerization temperature was maintained below 240 °C. Before the end of the reaction, the temperature was raised to 270 °C for 1 h to obtain higher molecular weight. The poly(ether ester) was purified by dissolving in chloroform and precipitating in excess methanol. The polymer was named PH31B32. The structures of the monomer and the polymer are represented in Figure 1.

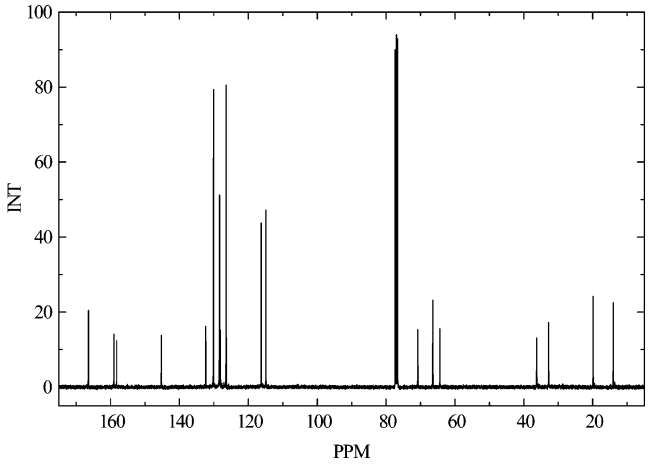

Figure 2. ^{13}C NMR spectrum of PH31B32 in deuterated chloroform.

^{1}H-RMN ($CDCl_3$): δ 1.18 (d, 3H, CH_2CH(C**H$_3$**)CH_2), 1.41 (d, 3H, CH(C**H$_3$**)CH_2CH_2), 2.07−2.29 (m, 2H, CH(CH_3)C**H$_2$**CH_2), 2.43−2.56 (m, 1H, CH_2C**H**(CH_3)CH_2), 4.10−4.23 (m, 2H, CH-(CH_3)CH_2C**H$_2$**), 4.38 (d, 4H, C**H$_2$**CH(CH_3)C**H$_2$**), 4.68−4.78 (m, 1H, C**H**(CH_3)CH_2CH_2), 6.92−8.08 (m, 16H, H_{ar}).

^{13}C-RMN ($CDCl_3$): δ 14.06 (CH_2CH(**C**H_3)CH_2), 19.89 (CH-(**C**H_3)CH_2CH_2), 32.82 (CH_2**C**H(CH_3)CH_2), 36.29 (CH(CH_3)**C**H_2-CH_2), 64.38 (CH(CH_3)CH_2**C**H_2), 66.45 (**C**$H_2CH(CH_3)$**C**H_2), 70.79 (**C**H(CH_3)CH_2CH_2), 114.91; 116.23; 126.43; 128.10; 128.11; 128.34; 128.41; 130.10; 132.37; 132.38; 145.20; 145.22; 158.22; 159.05 (24C_{ar}); 166.41 (**C**O$OCH_2CH(CH_3)$).

Experimental Methods. Solution-NMR measurements were carried out in a Varian 300 spectrometer, in deuterated chloroform at room temperature. Figure 2 shows the ^{13}C NMR spectrum of the PH31B32 sample.

The intrinsic viscosity of the polymer was measured at 30 °C in chloroform by using an Ubbelohde viscometer. A value of $[\eta]$ = 0.681 (dL/g) was found for the PH31B32 sample.

Size-exclusion chromatography data were obtained using a Waters 150C gel permeation chromatograph, equipped with two detectors: the conventional refractive index concentration detector and a viscometer Retrofit GPC 150R from Viscotek Co. The dual detection and universal calibration (obtained from measurements in different polystyrene standards using chloroform as eluent at 25 °C) allow one to determine absolute molecular weight values. The peak molecular weight value obtained for PH31B32 was M_p=12 000.

A film of the polymer was obtained by compression molding in a Collin press between hot plates (180 °C) at a pressure of 1.5 MPa and subsequently cooling to room temperature between water-cooled plates in press. This sample is named as quenched PH31B32. Several specimens were cut from this film and annealed in an oil bath at different temperatures and

times. However, the experiments for the annealing temperature of 115 °C and different times were performed inside the calorimeter.

Oriented fibers were obtained after annealing at 115 °C for 20 h in an oil bath and then by uniaxial stretching in a Minimat dinamometer at the same temperature and with a rate of 0.29 min^{-1}.

Differential scanning calorimetric measurements were carried out with a Perkin-Elmer DSC7 calorimeter connected to a cooling system. Samples of 6−9 mg were used at a heating rate of 20 °C/min.

Variable-temperature X-ray scattering experiments were performed by employing synchrotron radiation ($\lambda = 0.150$ nm) in the beamline A2 at HASYLAB (Hamburg, Germany). Two linear position-sensitive detectors were used simultaneously, one of them fixed and covering the approximate 2θ range from 10° to 30° and the other being set at two different sample−detector positions (in the direction of the beam): 43 and 225 cm, respectively. The first position covers the approximate 2θ range from 1.1° to 8.8° (spacings from 8 to 1 nm) and the second from about 0.18° to 1.6° (spacings from about 50 to 5.5 nm). Therefore, wide- (WAXS), middle- (MAXS), and small-angle scattering (SAXS) data are collected in the two experimental setups: simultaneous WAXS/MAXS profiles are acquired in the first case and WAXS/SAXS in the second.

Film samples, of about 20 mg, were covered by aluminum foil to ensure homogeneous heating or cooling and placed in the temperature controller of the line, under vacuum. Heating experiments were performed at a rate of 8 °C/min. The same temperature program was reproduced in the two setups, and the WAXS data were used to monitor the reproducibility of the results. The reproducibility was found to be well inside the inherent experimental resolution of the system.

The scattering patterns were collected in time frames of 30 s, so that we have a temperature resolution of 4 °C between frames. The calibration of the spacings for the different detectors and positions were made as follows: the diffractions of a crystalline PET sample were used for the WAXS detector; a sample of silver behenate (giving a well-defined diffraction at a spacing of 5.838 nm and several orders) was used for the MAXS detector; and the different orders of the long spacing of rat-tail cornea ($L = 65$ nm) for the SAXS detector.

The wide-angle X-ray diffraction photograph corresponding to the quenched polymer was taken, at room temperature, with a flat plate camera attached to a Phillips 2 kW tube X-ray generator using nickel-filtered Cu Kα radiation. The distance from sample to film was determined by using aluminum foil as standard.

The two-dimensional diffraction pattern for the stretched annealed specimen of PH31B32 was obtained in the synchrotron beamline, by using an image plate detector, located at a distance of 20.5 cm from the sample.

Results and Discussion

Thermal Properties. The DSC cooling and heating curves of PH31B32 are shown in the upper part of Figure 3. They show only a glass transition, centered at 95 °C on heating, and no other transition is observed at the usual DSC rates. As will be verified below, this corresponds to the glass transition of the amorphous phase of the polymer, i.e., at room temperature PH31B32 is an amorphous glass.

However, when the polymer is annealed at temperatures somewhat above the glass transition, some ordering is attained in the sample (a smectic liquid-crystalline mesophase, as will be deduced below). Thus, the lower part of Figure 3 presents the DSC heating curves corresponding to a specimen of PH31B32 after annealing at a temperature of 115 °C for different times. Two important features can be observed. First, an endotherm at around 145 °C is seen, with an intensity

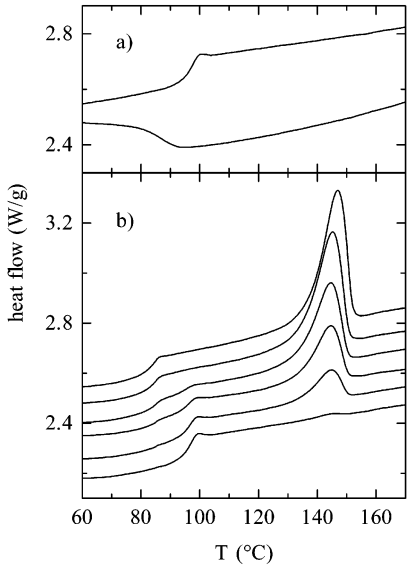

Figure 3. DSC curves corresponding to PH31B32: (a) cooling from the isotropic melt (bottom curve) and subsequent melting (top curve); (b) melting curves corresponding to a specimen of PH31B32 annealed at 115 °C for different times (from bottom to top: 15, 30, 37, 45, 60, and 120 min). Scanning rate, 20 °C/min.

that increases with the annealing time, although its position remains almost constant. Second, the glass-transition region depends also very much on the annealing time, showing a very interesting behavior: it is clearly composed of two differentiated processes, one of them centered at around 95 °C and the other at around 84 °C. Both components depend on the annealing time, the high-temperature one decreasing its intensity (its increment of associated specific heat) and the low-temperature one increasing with increasing annealing time.

These experiments suggest that an ordering process takes place in the polymer by annealing at that temperature. The process takes approximately 2 h to be completed, so that at lower annealing times the two phases (the amorphous phase and the ordered one) coexist, each leading to a different glass transition.

The two glass transitions can be more clearly identified in the corresponding first derivatives of the specific heat curves. These derivatives, in the region of the glass transitions, are shown in Figure 4. The two maxima, centered at around 84 and 95 °C, are clearly observed, corresponding to the inflection points in the specific heat increment at the glass transition. The maximum at 95 °C (the amorphous component) decreases in intensity with increasing annealing times, while the one at 84 °C (the "ordered" component) increases.

Taking into account that the glass transition is related to the freezing of segmental motions and that liquid-crystalline phases retain some mobility around the longitudinal axes of the mesogen, it seems reasonable to expect a glass transition of the liquid-crystalline phase at the temperature at which the minimum free volume required for the rotations is approached. The glass-transition temperature of polymers is closely related to the flexibility of the chains in the sense that a high value of T_g is generally assumed to be connected with relatively high barriers of bond rotations. These barriers depend not only on the type of bond, but also on the intermolecular constraint and therefore on the supramolecular arrangement of the chains. For this

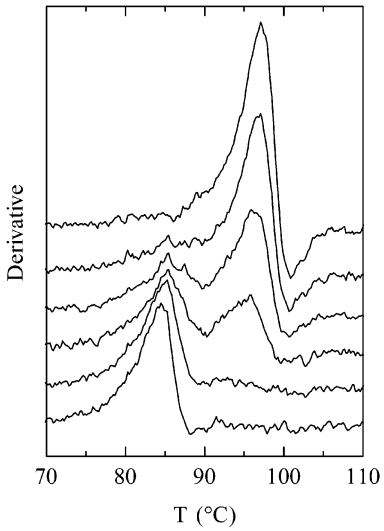

Figure 4. First derivative, in the glass-transition region, of the DSC melting curves in Figure 3b corresponding to the specimen of PH31B32 annealed at 115 °C for different times (from bottom to top: 120, 60, 45, 37, 30, and 15 min).

reason the glass-transition temperature of the liquid-crystalline phase can differ from that of the amorphous phase. Conformational analysis and X-ray diffraction indicate that highly extended conformers predominate in the LC phase.[15−17] Segmental movements above the glass transition in the LC phase shall not modify this orientation significantly, being therefore more restricted than in the amorphous state. The free volume necessary to perform these rotations is considerably smaller than the volume for segmental motion in the isotropic melt. Consequently, according to the free volume theory, the glass transition of the LC phase is reached at lower temperatures than the glass transition of the isotropic state.[6,7]

An additional interesting feature is observed in the derivatives of Figure 4: there is a region in the high-temperature part of both glass transitions where the derivatives take negative values. This is more evident in the amorphous component, but it is also observed in the other one. The origin of this feature is the enthalpy relaxation (aging process) of the material. The aging process is well documented in the amorphous regions of polymers,[22−24] but we also observed and analyzed it in liquid-crystalline phases.[25,26]

The present system constitutes a very good model to analyze the enthalpy relaxation separately in the amorphous and liquid-crystalline phases to investigate possible analogies or differences between the two phases. We plan to analyze this aspect soon.

To determine the nature of the phases involved, X-ray diffraction experiments on film samples were performed. Thus, Figure 5a represents the X-ray photograph of a film of PH31B32 quenched from melt. Only the amorphous halo is observed, centered at around 0.47 nm. Another specimen of PH31B32 was annealed during 20 h at 115 °C and then stretched in a Minimat dinamometer at the same temperature and with a rate of 0.29 min^{-1}. The presence of sharp inner reflections and broad outer reflections in the X-ray photograph (Figure 5b) suggests the appearance of a smectic phase with the mesogens distributed in layers lacking in-plane symmetry. The two inner spots appear at 1.26 and 0.63 nm. They are located on the meridional plane, indicating that the layer periodicity is aligned with the drawn

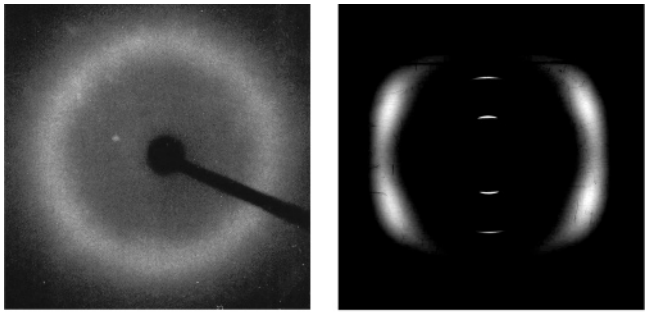

Figure 5. X-ray fiber diffractograms of PH31B32: (a) quenched isotropic sample; (b) specimen annealed at 115 °C for 20 h and stretched at the same temperature at 0.29 min^{-1}. Stretching direction, vertical.

direction and, consequently, the polymer chains are aligned along the fiber axis. The two diffuse outer reflections are split at both sides of the equator, forming an angle of 27°. These features are characteristic of a smectic SmCalt phase, where the mesogens are tilted with respect to the layer plane and the tilt direction alternates in successive layers.[18,27]

The extended chain length of the chemical repetitive unit, L, for PH31B32 is calculated to be 2.89 nm, but as depicted in Figure 1, the spacers between the biphenyl groups are different: besides the position of the methyl substituent, the spacer with the two ether linkages has a length of 1.28 nm, while that including the two ester groups amounts to 1.61 nm. We are dealing, therefore, with two alternating spacers of different length. Previous works on this kind of system[28,29] show that when the difference in length of the spacers is not very big, a single-layer smectic structure is obtained, as a result of the random mixing and accommodation of the two spacers. Such behavior is characterized by the obtainment of a smectic layer spacing around one-half of the total length of the repeat unit. As shown above, this is the case for PH31B32.

Therefore, the structure produced after annealing PH31B32 corresponds to a smectic SmCalt phase, i.e., a low-ordered mesophase. The rather slow rate of formation of this mesophase allows one to obtain samples with different degrees of liquid crystallinity just by adjusting the annealing time and then quenching to room temperature. The extent of the transformation can be deduced from the DSC curves in Figure 3. The evolution of different parameters (glass-transition temperature of the two phases, isotropization enthalpy, ΔH_i, and isotropization temperature, T_i) with the annealing time, t_a, is shown in Figure 6. It can be observed that ΔH_i increases very clearly with t_a, reaching an asymptotic value of 17 J/g at around 120 min. On the contrary, T_i and the two T_g's are practically constant with the annealing time, although the increment of specific heat, ΔC_p, associated to each of the phases is also clearly dependent on t_a, as shown in the upper part of Figure 7. Therefore, all three magnitudes, ΔH_i, and the two specific heat increments can be used to monitor the degree of transformation as it is represented in the lower part of Figure 7. Rather similar values of the "rate" of transformation are deduced from ΔH_i and from the ΔC_p's. It has to be considered that the sensitivity on the values of ΔH_i is much higher than in the other two magnitudes, which involve a considerably higher uncertainty on their determination.

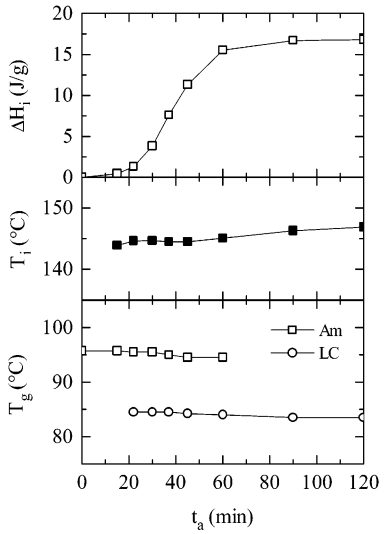

Figure 6. Variation of the isotropization enthalpy (upper), isotropization temperature (middle), and glass-transition temperatures of the two phases (lower) as a function of the annealing time for the PH31B32 specimen annealed at 115 °C.

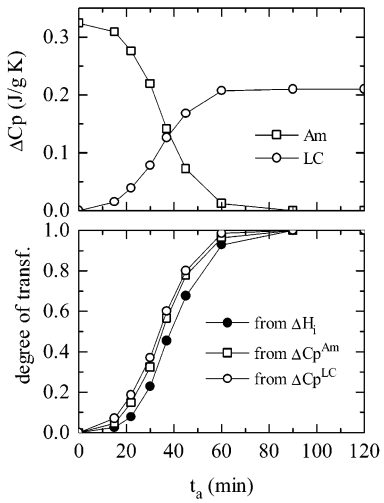

Figure 7. Variation of the increment of specific heat at the two different glass transitions (upper) and degree of transformation deduced from the isotropization enthalpy and from the two specific heat increments (lower) as a function of the annealing time for the PH31B32 specimen annealed at 115 °C.

That similarity and the fact that the value of ΔC_p for the amorphous component goes to zero at high annealing times, when the transformation is complete, is a rather strong argument in favor of considering that the mesophase formation is a process that reaches practically 100% of the material volume, in contrast to the reduced amount of crystallinity attained by regular semicrystalline polymers. That 100% of liquid crystallinity seems to be true at least in the present case of PH31B32, but we believe that it is a rather general case in mesophase-forming polymers (at least when low-ordered mesophases are involved). However, if this is the case, we are faced with the problem of the possible existence of chain entanglements and chain defects in general. We will come back to this issue on the basis of synchrotron experiments.

Additional experiments were performed on PH31B32 by annealing at different temperatures. Thus, Figure 8 shows the DSC melting curves corresponding to different specimens of PH31B32 annealed at the indicated temperatures and times. It has to be considered that the observed maximum rate of transformation occurs at annealing temperatures around 115 °C, so that the rate decreases at both higher and lower temperatures and considerably high annealing times are necessary if the departure from that temperature of the maximum is relatively big. Anyway, two facts are rather evident from Figure 8. First, the glass-transition temperature is practically constant, around 84 °C in all cases. Second, the isotropization peak, although keeping a fairly constant enthalpy, moves to higher temperatures as the annealing temperature is higher. These aspects are more clearly observed in Figure 9. Thus, the lower part shows the practical constancy of the glass-transition temperature, and the same seems to be true for the enthalpy of isotropization (middle part of Figure 9): the fact that a maximum at intermediate temperatures seems to be observed can be explained by the fact that the transformation may have not been complete for the annealing temperatures in the two extremes. We believe that ΔH_i would be practically constant, or slightly increasing, if the liquid-crystal formation were complete.

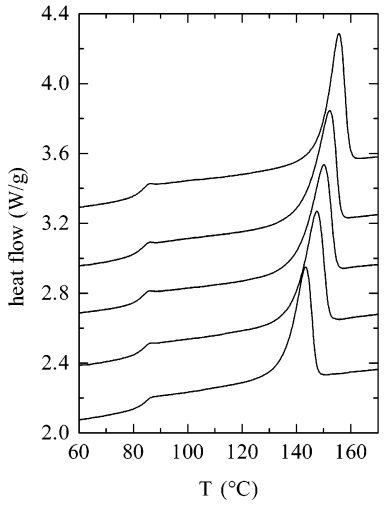

Figure 8. DSC melting curves corresponding to PH31B32 specimens annealed at different temperatures and times (from bottom to top: 43 h at 100 °C, 17 h at 110 °C, 17 h at 115 °C, 17 h at 120 °C, and 88 h at 130 °C). Scanning rate, 20 °C/min.

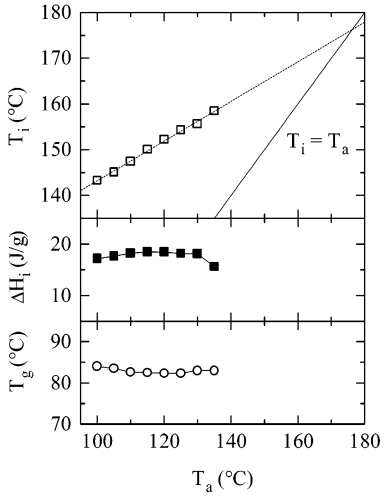

Figure 9. Variation of the isotropization temperature (upper), isotropization enthalpy (middle), and glass-transition temperature (lower) as a function of the annealing temperature.

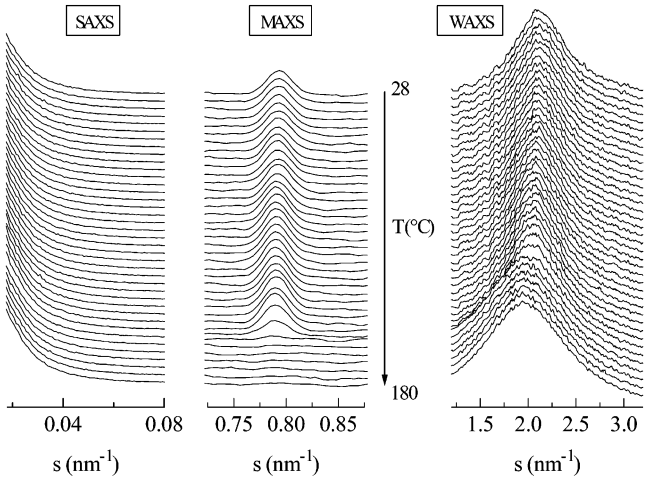

Figure 10. SAXS/MAXS/WAXS synchrotron profiles corresponding to a melting experiment of a PH31B32 specimen annealed for 88 h at 130 °C. Scanning rate, 8 °C/min.

More interesting is the behavior of the isotropization temperature, which shows a linear increase with the annealing temperature, as shown in the upper part of Figure 9. In fact, the slope of the linear fit shown in that figure is 0.43. This clear variation resembles somehow the well documented dependence of the melting temperature on the crystallization temperature of semicrystalline polymers. However, the explanation for that variation has to be different: in the case of semicrystalline polymers, it is due the finite size of the crystals, owing mainly to chain folding, with the subsequent surface free energy effects on the crystallites.[30–32] In the present case of a liquid-crystalline structure, we mentioned above that the mesophase seems to involve practically 100% of the material and, as we will discuss below, there seems to be no extensive chain folding. The variation of T_i may be explained, then, by a corresponding variation in the segregation of defects from the smectic structure, leading to higher correlation lengths. When discussing below the synchrotron results, we will present more arguments on this issue.

Independent of the origin of that increase, the fitted straight line to the T_i variation intercepts the line $T_i = T_a$ at around 176 °C, as observed in the upper part of Figure 9. It seems, therefore, that the "equilibrium" isotropization temperature for PH31B32 is around 176 °C, if the mesophase were allowed to be formed at sufficiently high temperatures and times.

Synchrotron Results. Three specimens of PH31B32, two of them annealed at 100 and 130 °C and another one quenched from melt, have been analyzed under real-time conditions by employing synchrotron radiation. The SAXS/MAXS/WAXS profiles for the melting of the specimen annealed at 130 °C are shown in Figure 10. At low temperatures, an amorphous-like wide halo is observed in the WAXS channels and a clear MAXS peak, corresponding to a spacing of 1.26 nm. These features are characteristic of a low-ordered mesophase, as correspond to a SmCalt phase assigned before. At high temperatures, above the isotropization point, the MAXS peak disappears and the WAXS halo moves slightly to lower *s* values (the results for the specimen annealed at 100 °C are qualitatively very similar, while, obviously, those for the quenched specimen do not present the MAXS peak).

The analysis of the intensities, positions, and widths of the peaks in those diffractograms allows one to obtain some important quantitative information. Thus, the MAXS results are presented in Figure 11, while the most relevant WAXS data are shown in Figure 12. The upper part of Figure 11 represents the variation with temperature of the position of the MAXS peak (obviously only for the two annealed specimens). It can be observed that the layer spacings for the specimen annealed at 100 °C are slightly higher than those for the one annealed at 130 °C. In fact, that spacing, at room temperature, takes the values of 1.267 and 1.260 nm, respectively, for the specimens annealed at 100 and 130 °C. The temperature variation is, however, very similar in the two cases, with an apparent temperature coefficient of $(5 \pm 2) \times 10^{-5}$ nm °C^{-1}.

These relative values of the layer spacing can be interpreted as a result of a slightly more compact structure in the case of the higher annealing temperature, probably associated to a lower configuration entropy, which may contribute somewhat to the higher isotropization temperature.

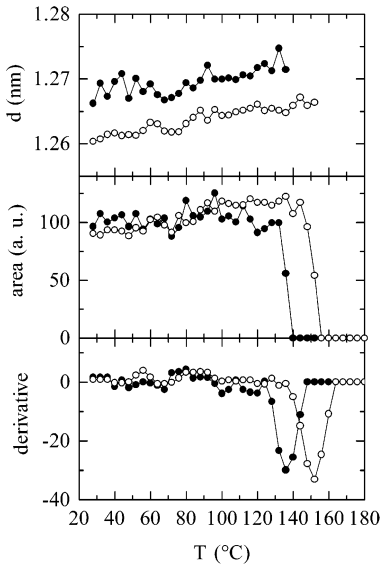

Figure 11. Temperature dependence, on melting, of different MAXS parameters corresponding to two specimens of PH31B32 annealed at 100 (solid symbols) and 130 °C (open symbols). From top to bottom: spacing of the MAXS peak, area of the MAXS peak, and derivative of this area.

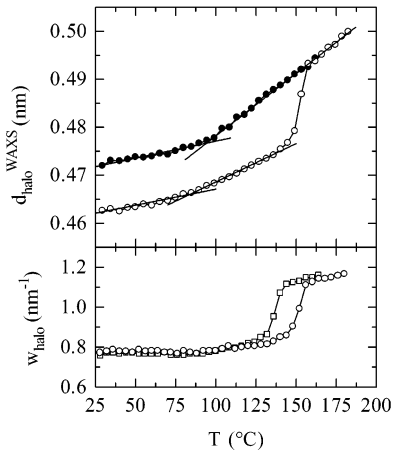

Figure 12. Temperature dependence, on melting, of the spacing corresponding to the WAXS broad peak (upper) and its width at half-height (lower) for different PH31B32 specimens: quenched (solid circles), annealed at 130 °C (open circles), and annealed at 100 °C (open squares).

The middle part of Figure 11 shows the variation with temperature of the intensity of the MAXS peak. The most interesting feature is the disappearance of the MAXS peak during the isotropization. The derivative of these intensities (lower part of Figure 11) allows one to locate very clearly the isotropization, which, for these MAXS data, occurs at 137 at 151 °C, respectively, which compares very well with the DSC data in Figures 8 and 9, especially when considering the differences in the heating rate.

Regarding the WAXS results, the more relevant data, related to the position of the amorphous-like WAXS peak, are displayed in the upper part of Figure 12, where the corresponding temperature variation for the specimen annealed at 130 °C is compared with that for the quenched sample. Two interesting features are noticeable. First, during the isotropization there is a rather significant change in the position of the WAXS peak, so that the most probable intermolecular distance between chains, which is directly related to the maximum of the WAXS peak,[33] is clearly smaller in the case of the liquid-crystalline phase in comparison with the isotropic state. Second, the temperature coefficients for the different phases involved can be determined from these data. It can be observed that the values for the isotropic state of the annealed specimen are obviously coincident with those of the quenched sample at high temperatures, i.e., above T_g. The corresponding apparent temperature coefficient takes the value of $(26 \pm 1) \times 10^{-5}$ nm °C^{-1}.

Below the isotropization, not only is the intermolecular distance in the annealed specimen smaller than the isotropic one, but also its temperature coefficient is significantly smaller: on the order of $(16 \pm 1) \times 10^{-5}$ nm °C^{-1}. At lower temperatures, below T_g, the two specimens have even lower temperature coefficients: the observed values are $(7 \pm 1) \times 10^{-5}$ nm °C^{-1} in both cases, i.e., the amorphous glass and the liquid-crystalline glass of PH31B32 seem to have the same temperature coefficient (the same expansion coefficient of the most probable intermolecular distance).

The glass-transition temperatures of these two kinds of glasses are, however, different, as deduced from the temperatures where the expansion coefficients change. These temperatures correspond to the intersections of the two fitting straight lines shown in Figure 12. The intersection points are 94 and 84 °C for the quenched and annealed specimens, respectively. These glass-transition temperatures, corresponding to the amorphous and liquid-crystalline states, are in perfect agreement with those commented on above deduced from DSC. These results obtained for the specimen annealed at 130 °C are totally coincident with those for the one annealed at 100 °C (with the exception, of course, of a different isotropization temperature).

The lower part of Figure 12 shows the variation with temperature of the width at half-height, w, of the WAXS peak for the two annealed PH31B32 specimens. Besides the small change of slope around 85 °C, i.e., around the glass transition of the mesophase, a rather clear increase of the width is also observed during the isotropization.

Therefore, these results indicate that although the WAXS profiles of the two phases (mesophase and amorphous) are rather similar, the mesophase has noticeably smaller most probable intermolecular distances and a smaller width of the WAXS broad peak.

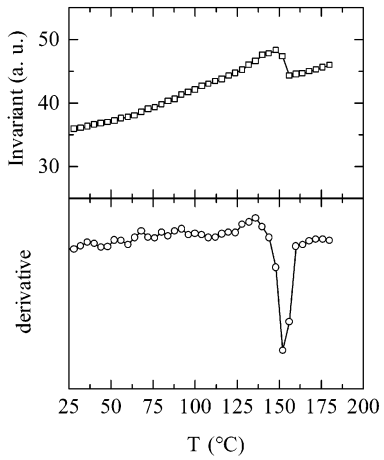

Figure 13. Temperature dependence, on melting, of the SAXS relative invariant (upper) and its derivative (lower) corresponding to the specimen of PH31B32 annealed at 130 °C.

The SAXS profiles corresponding to a melting experiment of the specimen annealed at 130 °C are also presented in Figure 10. No clear long spacing is observed at any temperature. Three interpretations can be given to explain the fact that no long spacing is observed in the mesophase. The first one is that the long spacing may be rather high and falls outside the detector's window. The second one is that there is not enough electronic difference between amorphous and liquid-crystalline regions or there is no periodicity between the two regions to be expressed in an observable long spacing. The third one is simply that the liquid-crystalline phase occupies 100% of the material volume (or nearly 100%), so that no long spacing can be derived from it. From the structural model for the smectic mesophase that will be presented below, the three interpretations may be somewhat realistic.

Although there is no appreciable long spacing, a rather subtle change on the SAXS profiles in Figure 10 is observed during the isotropization. This small change is more clearly reflected on the variation of the relative SAXS invariant,[34–36] which shows a clear discontinuity during the isotropization of the sample, as observed in the upper part of Figure 13. Its derivative (lower part of Figure 13) has a minimum centered at around 152 °C, in perfect agreement with the MAXS results in Figure 11.

The SAXS invariant is a magnitude used in the lamellar stack model theory of semicrystalline polymers which is directly related to the electron density differences between the two phases (amorphous and crystalline), so that it has rather important variations during crystallization, recrystallization, or melting processes in semicrystalline polymers or in the case of liquid-crystalline polymers when highly ordered phases are involved.[37] The very small change observed in the present case of PH31B32, together with the improbable existence of a periodic stacked structure in its mesophase, may be due just to differences in the density fluctuations of the two pure phases.

A final issue from the synchrotron results refers to the correlation length, D, of the mesophase, which can be estimated from the width of the MAXS peak and a simple application of the Scherrer equation. Thus, the width at half-height of the MAXS peak in Figure 10 is approximately constant with temperature, taking an average value of 0.019 nm^{-1}, which means a correlation

length on the order of 50 nm, which has to be considered as a lower limit since corrections for neither the experimental broadening nor the possible existence of internal defects[34] have been made. The MAXS peak for the sample annealed at 100 °C is slightly wider, and a correlation length of around 41 nm is deduced from it.

On the other hand, the present sample of PH31B32 was found to have a molecular weight value which comprises around 22 monomeric units, i.e., the extended length of an average chain is around 63 nm. From these considerations, it follows that the correlation lengths are on the order of the extended chain length of the polymer, so that no extensive chain folding seems to be present in the liquid-crystalline state of PH31B32. Dealing with extended chains, the result of a 100% (or nearly) liquid crystallinity appears to be more reasonable, since the not very high molecular weights involved should lead to not many entanglements, so that the degree of liquid crystallinity can reach a value very close to 100%. Previous results[38,39] on a sample of poly(heptamethylene *p*,*p*′-bibenzoate) also concluded that the correlation length was on the order of the extended chain length, in this case for a sample of higher molecular weight M_n of 16 200, with an intrinsic viscosity of 1.03 dL g^{-1}. Since the usual molecular weights of similar liquid-crystalline polymers are not very high and in fact it is unusual to report intrinsic viscosities higher than 1 dL g^{-1}, it follows that we may deal with almost extended chains in the low-ordered mesophases of these and similar liquid-crystalline polymers.

In addition, it seems that the correlation length depends on the annealing temperature, obtaining higher values of that parameter for the higher annealing temperatures. This may be directly related to the variation of the isotropization temperature. Thus, the proposed hierarchical structural model for smectic mesophases[40,41] consists of more or less extended chains assembled with the mesogens disposed into smectic layers oriented perpendicular to the chain axis. Stacks of these smectic layers are then organized in lamellae-like structures of several tens of nanometers whose regular stacking is disrupted by regions where the different defects (chain ends, some folds and entanglements, and other defects[42]) are contained. However, these disordered regions shall be composed of a relatively low amount of material since the above-mentioned results point to an almost 100% liquid-crystalline polymer. With this picture, the variation of the isotropization temperature for PH31B32 can be explained by the fact that higher annealing temperatures will lead to a greater segregation of those defects from the smectic structure, attaining higher correlation lengths.

Conclusions

It has been found that the poly(etherester) PH31B32 develops a low-ordered SmCalt mesophase with a rather slow rate of formation in such a way that the isotropic melt of this polymer can be easily quenched into the glassy amorphous state at the usual cooling rates of the calorimeter. Considerably high annealing times at temperatures above T_g are necessary to develop such mesophase. The extent of the transformation and the symmetry of the mesophase have been determined by means of calorimetric and X-ray diffraction experiments. The DSC results show that the glass-transition temperatures of the amorphous and liquid-crystalline states are clearly different: 95 and 84 °C, respectively. Moreover, the results show that the isotropization temperature increases linearly with the annealing temperature (the temperature at which the mesophase has been formed).

Additional structural results have been obtained from real-time variable-temperature synchrotron experiments. Thus, the mesophase layer spacing is slightly lower for the higher annealing temperatures, indicating a slightly more compact structure. Moreover, although the WAXS profiles of the two phases (mesophase and amorphous) are rather similar, the mesophase has noticeably smaller most probable intermolecular distances and a smaller width of the WAXS broad peak. The temperature coefficients of these intermolecular distances are also different for the various phases, and clear discontinuities are observed at the glass transitions. The corresponding values of T_g obtained from these results are 94 and 84 °C for the amorphous and liquid-crystalline phases, respectively, in perfect agreement with the DSC results.

The correlation lengths estimated from the widths of the mesophase layer peaks are on the order of the extended chain length of the polymer, so that no extensive chain folding seems to be present in the mesophase of PH31B32. This fact will favor the attainment of high degrees of liquid crystallinity, which in the present case seems to be practically 100%. Moreover, the higher correlation lengths deduced for the higher annealing temperatures point to a segregation of defects from the smectic structure in a greater extent, which may explain the corresponding higher isotropization temperatures.

Acknowledgment. The financial support of MCYT (Project MAT2001-1731) is gratefully acknowledged. J.P.F.-B. Is indebted to CSIC for a research grant financed by the I3P program through the *Fondo Social Europeo*. The synchrotron work was supported by the EU (Contracts HPRI-CT-1999-00040/2001-00140). We thank the collaboration of the Hasylab personnel, especially Dr. S. Funari, responsible for the polymer beamline.

References and Notes

(1) MacDonald, W. A. In *Liquid Crystal Polymers: From Structures to Applications*; Elsevier: New York, 1992; Chapter 8, p 407.
(2) Brand, H. R.; Finkelmann, H. In *Handbook of Liquid Crystals*; Demus, D., Goodby, J., Gray, G. W., Spiess, H. W., Vill, V., Eds.; Wiley-VCH: New York, 1998; Vol 3.
(3) Frosini, V.; de Petris, S.; Chiellini, E.; Galli, G.; Lenz, R. W. *Mol. Cryst. Liq. Cryst.* **1983**, *98*, 223.
(4) Gómez, M. A.; Marco, C.; Fatou, J. M. G.; Suárez, N.; Laredo, E.; Bello, A. *J. Polym. Sci., Part B: Polym. Phys.* **1995**, *33*, 1259.
(5) Tokita, M.; Osada, K.; Watanabe, J. *Polym. J.* **1998**, *30*, 589.
(6) Chen, D.; Zachmann, H. G. *Polymer* **1991**, *32*, 1612.
(7) Ahumada, O.; Ezquerra, T. A.; Nogales, A.; Baltá-Calleja, F. J.; Zachmann, H. G. *Macromolecules* **1996**, *29*, 5002.
(8) del Campo, A.; Bello, A.; Pérez, E.; García-Bernabé, A.; Díaz-Calleja, R. *Macromol. Chem. Phys.* **2002**, *203*, 2508.
(9) García-Bernabé, A.; Díaz-Calleja, R.; Sanchis, M. J.; del Campo, A.; Bello, A.; Pérez, E. *Polymer* **2004**, *45*, 1533.
(10) Watanabe, J.; Hayashi, M. *Macromolecules* **1988**, *21*, 278.
(11) Watanabe, J.; Hayashi, M. *Macromolecules* **1989**, *22*, 4083.
(12) Watanabe, J.; Kinoshita, S. *J. Phys. II Fr.* **1992**, *2*, 1237.
(13) (a) Pérez, E.; Pereña, J. M.; Benavente, R.; Bello, A. Characterization and Properties of Thermotropic Polybibenzoates. In *Handbook of Engineering Polymeric Materials*; Cheremisinoff, N. P., Ed.; Marcel Dekker: New York, 1997; Chapter 25, p 383. (b) Pérez, E. Liquid crystalline polymers: Polyesters of bibenzoic acid. In *The Polymeric Materials Encyclo-*

pedia; Salamone, J. C., Ed.; CRC Press: Boca Raton, FL, 1996; Vol. 5, p 3711.
(14) Nakata, Y.; Watanabe, J. *Polym. J.* **1997**, *29*, 193.
(15) Abe, A. *Macromolecules* **1984**, *17*, 2280.
(16) Pérez, E.; Riande, E.; Bello, A.; Benavente, R.; Pereña, J. M. *Macromolecules* **1992**, *25*, 605.
(17) Bello, A.; Riande, E.; Pérez, E.; Marugán, M. M.; Pereña, J. M. *Macromolecules* **1993**, *26*, 1072.
(18) Pérez, E.; Benavente, R.; Cerrada, M. L.; Bello, A.; Pereña, J. M. *Macromol. Chem. Phys.* **2003**, *204*, 2155.
(19) del Campo, A.; Pérez, E.; Benavente, R.; Bello, A.; Pereña, J. M. *Polymer* **1998**, *39*, 3847.
(20) Watanabe, J.; Hayashi, M.; Kinoshita, S.; Niori, T. *Polym. J.* **1992**, *24*, 597.
(21) Mitsunobu, O. *Synthesis* **1981**, 1.
(22) Struik, L. C. E. *Physical aging of amorphous polymers and other materials*; Elsevier: Amsterdam, 1978.
(23) Tant, M. R.; Wilkes, L. *Polym. Eng. Sci.* **1981**, *21*, 874.
(24) McKenna, G. B. In *Comprehensive Polymer Science;* Booth, C., Price, C., Eds.; Pergamon: Oxford, 1990; Vol. 2 (Polymer Properties), p 311.
(25) Lorenzo, V.; Pereña, J. M.; Pérez, E.; Benavente, R.; Bello, A. *J. Mater. Sci.* **1997**, *32*, 3601.
(26) Pérez, E.; Pereña, J. M.; Benavente, R.; Bello, A.; Lorenzo, V. *Polym. Bull.* **1992**, *29*, 233.
(27) Tokita, M.; Osada, K.; Watanabe, J. *Liq. Cryst.* **1997**, *24*, 477.
(28) Watanabe, J.; Nakata, Y.; Simizu, K. *J. Phys. II Fr.* **1994**, *4*, 581.
(29) Watanabe, J.; Hayashi, M.; Nakata, Y.; Niori, T.; Tokita, M. *Prog. Polym. Sci.* **1997**, *22*, 1053.
(30) Mandelkern, L. *Crystallization of Polymers;* McGraw-Hill: New York, 1964.
(31) Hoffman, J. D.; Weeks, J. J. *J. Res. Natl. Bur. Stand.* **1962**, *66A*, 13.
(32) Wunderlich, B. *Macromolecular Physics*; Academic Press: New York, 1980; Vol. 3.
(33) Klug, H. P.; Alexander, L. E. *X-ray Diffraction Procedures for Polycrystalline and Amorphous Materials*; Wiley: New York, 1954; p 632.
(34) Baltá-Calleja, F. J.; Vonk, C. G. *X-ray Scattering of Synthetic Polymers*; Elsevier: Amsterdam, 1989.
(35) Ryan, A. J.; Stanford, J. L.; Bras, W.; Nye, T. M. W. *Polymer* **1997**, *38*, 759.
(36) Crist, B. *J. Polym. Sci., Part B: Polym. Phys.* **2001**, *39*, 2454.
(37) Pérez, E.; del Campo, A.; Bello, A.; Benavente, R. *Macromolecules* **2000**, *33*, 3023.
(38) Pérez, E.; Todorova, G.; Krasteva, M.; Pereña, J. M.; Bello, A.; Marugán, M. M.; Shlouf, M. *Macromol. Chem. Phys.* **2003**, *204*, 1791.
(39) Todorova, G. K.; Krasteva, M. N.; Pérez, E.; Pereña, J. M.; Bello, A. *Macromolecules* **2004**, *37*, 118.
(40) Hu, Y. S.; Schiraldi, D. A.; Hiltner, A.; Baer, E. *Macromolecules* **2003**, *36*, 3606.
(41) Tsukruk, V. V.; Shilov, V. V.; Lipatov, Y. S. *Acta Polym.* **1985**, *36*, 403.
(42) Kléman, M. Defects and Textures in Liquid Crystalline Polymers. In *Liquid Crystallinity in Polymers: Principles and Fundamental Properties*; Ciferri, A., Ed.; VCH Publishers: New York, 1991; Chapter 10, p 365.

MA049354R